

This article was downloaded by: [Tomsk State University of Control Systems and Radio]

On: 21 February 2013, At: 10:35

Publisher: Taylor & Francis

Informa Ltd Registered in England and Wales Registered Number: 1072954
Registered office: Mortimer House, 37-41 Mortimer Street, London W1T 3JH, UK



Molecular Crystals and Liquid Crystals

Publication details, including instructions for authors and subscription information:

<http://www.tandfonline.com/loi/gmcl16>

Observations of Electrically Surface-Induced Regular Arrays of Focal Conies in a Homeotropic NPOB Smectic A Liquid Crystal

H. P. Hinov^a, N. Shonova^a & K. Avramova^a

^a Institute of Solid State Physics, Boul. Lenin 72, Sofia, 1184, Bulgaria

Version of record first published: 17 Oct 2011.

To cite this article: H. P. Hinov, N. Shonova & K. Avramova (1983): Observations of Electrically Surface-Induced Regular Arrays of Focal Conies in a Homeotropic NPOB Smectic A Liquid Crystal, *Molecular Crystals and Liquid Crystals*, 97:1, 297-315

To link to this article: <http://dx.doi.org/10.1080/00268948308073159>

PLEASE SCROLL DOWN FOR ARTICLE

Full terms and conditions of use: <http://www.tandfonline.com/page/terms-and-conditions>

This article may be used for research, teaching, and private study purposes. Any substantial or systematic reproduction, redistribution, reselling, loan, sub-licensing, systematic supply, or distribution in any form to anyone is expressly forbidden.

The publisher does not give any warranty express or implied or make any representation that the contents will be complete or accurate or up to date. The accuracy of any instructions, formulae, and drug doses should be

independently verified with primary sources. The publisher shall not be liable for any loss, actions, claims, proceedings, demand, or costs or damages whatsoever or howsoever caused arising directly or indirectly in connection with or arising out of the use of this material.

Observations of Electrically Surface-Induced Regular Arrays of Focal Conics in a Homeotropic NPOB Smectic A Liquid Crystal*

H. P. HINOV, N. SHONOVA and K. AVRAMOVA

Institute of Solid State Physics, Boul. Lenin 72, Sofia 1184, Bulgaria

Regular arrays of confocal pairs of ellipse-hyperbola with Marignan-Malet-Parodi association were observed in the boundary regions of a smectic A NPOB liquid crystal after cooling of a homeotropic nematic layer subjected to the action of a transversal high-frequency electric field with a sufficient strength. These smectic A textures exist as a storage mode after the removal of the electric field. Their distribution and sizes depend on the surface energy which has been determined to be in the range of 5×10^{-3} erg/cm² for a clear or lecithin-coated glass plate. In hybrid-aligned planar-homeotropic smectic A layers under the same conditions simultaneously exist parabolic focals and edge-dislocations near the glass plate where the surface orientation is planar and regular arrays of confocal pairs of ellipse-hyperbola near the glass plate where the surface orientation is homeotropic. The regular arrays of confocal domains might be used as diffraction gratings whereas the nonregular strong-scattering arrays obtained at lower electric fields might be used in the indicator technique.

I. INTRODUCTION

The various smectic (Sm) phases are usually obtained and investigated after a slow cooling of a well-aligned nematic (N) phase (in the cases when it exists) down to the smectic phase. In this way, well-aligned smectics are created. However, a Sm phase can be created also by a slow or rapid cooling of a previously deformed nematic phase. This manner of a sample preparation permits both the creation of various Sm scattering textures which are useful for industrial applications¹⁻³ and the study of the Sm surface forces, insufficiently investigated up to now, which are impor-

*This paper was presented at Ninth International Liquid Crystal Conference, Bangalore, India, December 6–10, 1982.

tant for the possible matching between the smectic surface and bulk orientations.²⁻⁵

It is worthwhile mentioning that the obtaining of useful Sm scattering textures and the investigation of the Sm surface forces can be realized either in the presence of a gradient in the transition temperature accompanied by the creation of well-defined pretransitional stripes¹⁻³ and closely related to the strength of the N deformations and to the rate of cooling or after freezing of the N realignment giving rise to a number of dislocations and/or disclinations which are often transformed into the energetically more favorable focal conics.

The Sm surface forces can be investigated in two ways: by a study of the various Sm textures obtained either in thin Sm films with a thickness below 10–15 μ under the action of well-defined surface forces⁵⁻⁹ or in the boundary regions under the competition between the surface orientation imposed by one of the cell boundaries and the bulk orientation imposed by magnetic and electric etc. torques or by a fluid flow.⁹⁻¹²

After the study of the matching between the planar surface orientation of a Sm A liquid crystal (LC) fixed by strong surface forces and the homeotropic orientation of the Sm A molecules in the bulk determined by electric forces,² our attention is focused now on the inverse case: the matching between the homeotropic (or slightly inclined) surface orientation of a Sm A LC and the planar orientation of the Sm A molecules in the bulk determined under the action of ac electric field torques. In effect this important and interesting problem has been investigated both theoretically^{13,14} and experimentally.¹⁵⁻¹⁷ The surface-bulk LC adaptation depends very strongly on the orientation of the Sm A molecules and the position of the Sm A planes in depth of the LC layer and can determine the creation of arrays of parabolic focal conics in the case of a slight undulation of initially planar Sm A layers,¹⁸ concentric rings of array defects when the planar Sm A layers are straight¹⁵ etc.

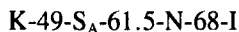
During our experimental investigations, a number of Sm A scattering textures, either already observed or being novel, were obtained due to the competition between the nearly homeotropic orientation of the molecules at the boundaries in the N and Sm A phases and the planar orientation of the N and Sm A phases in the bulk which is achieved under the action of a high-frequency transversal electric field.

We present a description of the performed experiment followed by the experimental results obtained and finally, propose a physical model which, in our opinion, can explain the main experimental results.

II. EXPERIMENTAL RESULTS

A. A compound and a sample preparation

The LC under study 4-nitrophenyl-4'-octyloxybenzoat (NPOB), with the following transition scheme (°C):¹⁹



has a strong tendency to a homeotropic orientation in the N and Sm A phases.

The isotropic phase of the LC was introduced between two carefully cleaned glass plates separated by two metal foils 10–50 μ thick. The cell was then heated from below on a special temperature regulator.

During the experimental investigations a number of homeotropic and hybrid-aligned planar-homeotropic NPOB films were cooled down to the Sm A phase in the presence of an ac transversal electric field with a different strength. The planar orientation of the LC molecules was achieved by SiO treatment of the glass plates under vacuum evaporation. The homeotropic orientation, on the other hand, was achieved either by a lecithin coating of the glass plates or by a careful cleaning of the glass plates.

B. Thermal distribution in the LC cells under investigation

From the simple technique of a sample heating one should expect a vertical temperature gradient directed from the lower to the upper glass plate. However, we surprisingly observed such a temperature gradient only in thick cells when the thickness was above 25 μ . This was evident by the creation of well-defined Cladis-Torza's stripes as well.¹ In thin cells, however, the temperature was equal inside the liquid crystal which was approximately revealed by the typical scattering properties of the widely used short-pitch cholesterics. For instance, the clear colors produced by such a cholesteric LC 10–20 μ thick and being heated from below unambiguously pointed out the nearly equal temperature over the entire LC layer—the temperature gradient would lead to the observation of iridescent colors, as has been calculated by Hajdo and Eringen.²⁰ One observes, however, a significant temperature gradient between the outer sides of the glass plates confining the LC, which clearly shows the great importance of the thermal properties of the glass plates depending on their thickness and thermal conductivity, etc.

C. An electric field application

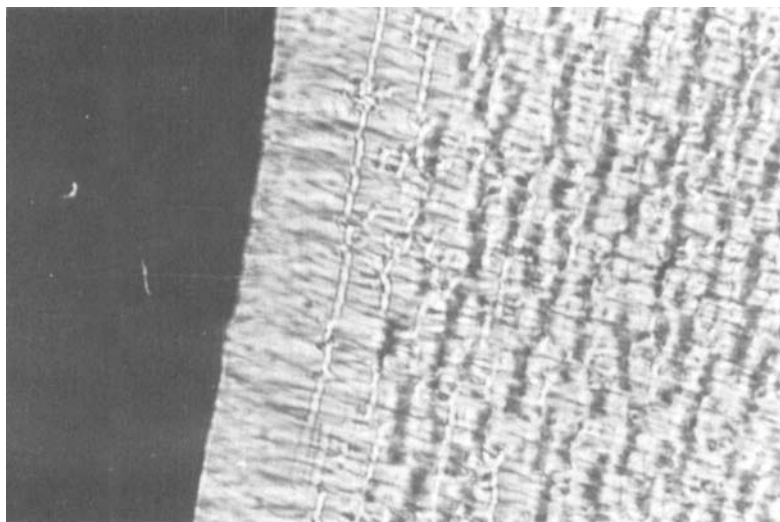
The dielectric properties of the NPOB LC under study in both the N and Sm A phases, as well the temperature dependence of the dielectric tensor elements, have been investigated by Barnik *et al.*²¹ Only a small variation in the dielectric anisotropy just below the I-N phase transition has been observed. Moreover, the value of the dielectric anisotropy of the N and Sm A phases has been determined to be around +15. In addition, the elastic and viscosity coefficients are also known.²¹

An ac electric field with a strength between E_{th} (the threshold electric field was in the range of 200–250 V/cm) and $35 E_{th}$ was applied across the LC films under study in both the N and Sm A phases in order to obtain a complete orientation of the N molecules in the middle part of the samples being parallel to the electric field direction (positive value of the dielectric anisotropy) and two strongly deformed LC nematic regions at the glass slides (one strongly deformed region in the hybrid-aligned cells). The frequency of the electric field ($f = 5$ kHz) was sufficiently high to ensure the orientating action of the dielectric torques without any hydrodynamic movement of the fluid.

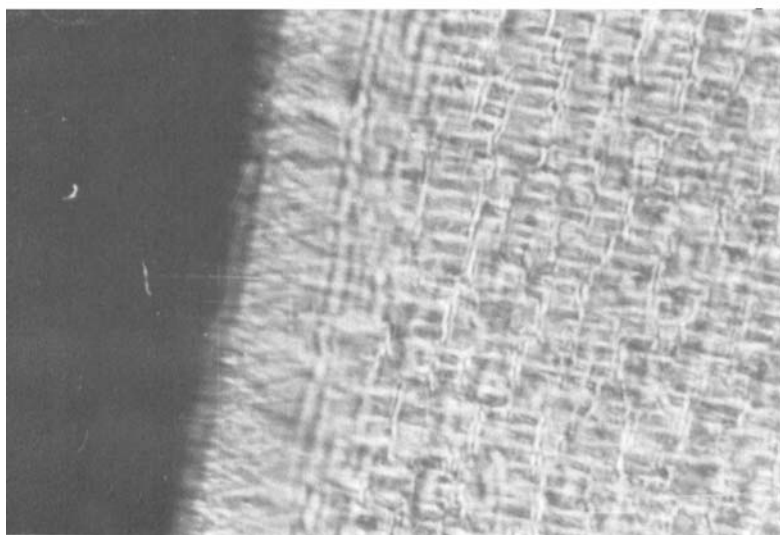
D. Microscopic observations

The application of an ac voltage in the range of 15–20 V (the distance between the metal foils was in the range of 1 mm) usually led to a Fréedericksz transition starting first around the metal foils and continuing to the middle part of the samples. This special appearance of the Fréedericksz transition is due to the inhomogeneous electric field, which is high around the metal foils and low in the middle part of the samples (in some of the cells under study the electric field was nearly homogeneous in the great part of the LC). This experimental finding was also confirmed by the directly observable movement of air bubbles under the electric field gradient torques.

The cooling of the N phase down to the Sm A phase in the presence of a relatively low voltage (around 100 V) led to the formation of a novel strongly scattering texture consisting of nonregular arrays of confocal domains (Figures 1a and 1b). The preliminary investigation of the scattering properties of this structure unambiguously showed a strong dependence on the nicol position. Raising the voltage above 200 V led to the formation of a typical Sm A texture which we called arrays of confocal domains (ACD) (Figure 2) (this Sm A texture has been obtained in NPOB by Köler,²² by Nesrullaev *et al.*¹² and Scudieri²³ in other ICs). On the other hand, this structure cannot be obtained around the electrodes or air bubbles (Figure 3)



(a)



(b)

FIGURE 1 Nonregular arrays of confocal domains in a NPOB Sm A film $10\ \mu$ thick; $U = 100\ \text{V}$, $f = 5\ \text{kHz}$ ($l = 1\ \text{mm}$), crossed nicols, the electric field is along the nicol bisectrice; the long side of the photo corresponds to $230\ \mu$. a) upper focusing and b) down focusing.

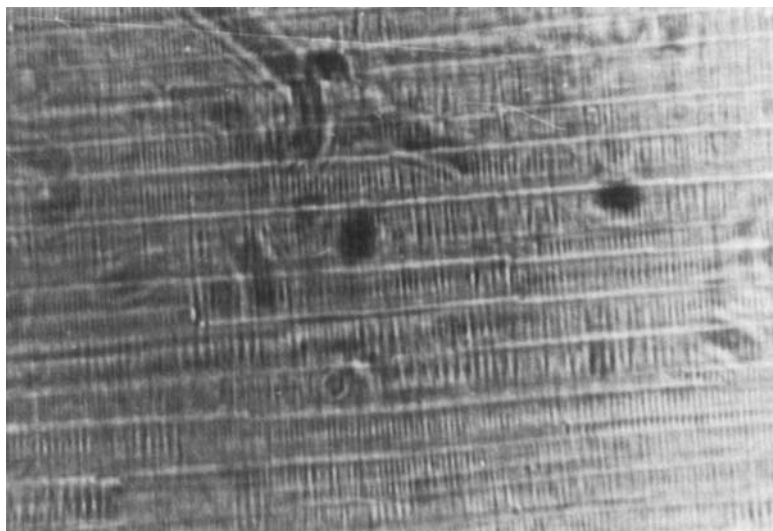


FIGURE 2 Regular arrays of confocal domains in a NPOB Sm A film $10\ \mu$ thick; $U = 400\ \text{V}$, $f = 5\ \text{kHz}$ ($l = 2.5\ \text{mm}$), crossed nicols, the electric field is along the nicol bisectrice; the long side of the photo corresponds to $230\ \mu$.

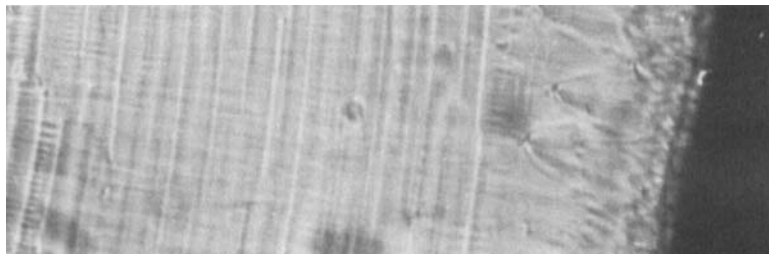


FIGURE 3 The regular arrays of confocal domains are formed usually far away from the electrodes; a NPOB Sm A film $10\ \mu$ thick, $U = 300\ \text{V}$, $f = 5\ \text{kHz}$ ($l = 1\ \text{mm}$), crossed nicols, the electric field is along the nicol bisectrice; the long side of the photo corresponds to $230\ \mu$.

possibly due to the different initial orientation of the N and Sm A molecules in these regions (let us note that according to Scudieri²³ the confocal domains in such arrays are not anchored whereas around air bubbles impurity centers exist which can prevent the formation of these arrays of focal conics). Instead of ACD we very often have seen many parabolic focals existing in the entire Sm A temperature interval and closely related to the nearly planar position of the Sm A molecules (vertical position of the

Sm A planes¹⁸). The optical picture of this Sm A texture strongly depends on the nicol position (the Sm A textures shown in Figures 2 and 3 were taken under crossed nicols and the electric field direction was along the nicol bisectrice). The great importance of the nicol position for the optical image of the confocal domains with ellipses situated in planes parallel or slightly inclined to the glass plates can be seen, for instance, from the excellent symmetric picture being found by Friedel in a drop of EMBAC (Figure 5 in Ref. 24). The slight rotation of one of the nicols, i.e. the rotation of the polarizer at an angle of about 10–15°, led to another important view of the ACD texture (Figure 4) which is useful since it directly reveals the confocal character of the arrays observed. On the other hand, the sample rotation up to the coincidence of the electric field direction with one of the nicols revealed another important view of the focal conics shown in Figures 5 and 6. In some regions of Figure 5, marked by us, one can see the exact position of confocal domains from two adjacent arrays. The preliminary optical investigations pointed out that this Sm A texture, typical for a high voltage excitation of the LC, is weakly scattering and does not significantly depend on the nicol position. However, this Sm A texture can be successfully applied for obtaining a good diffraction grating.

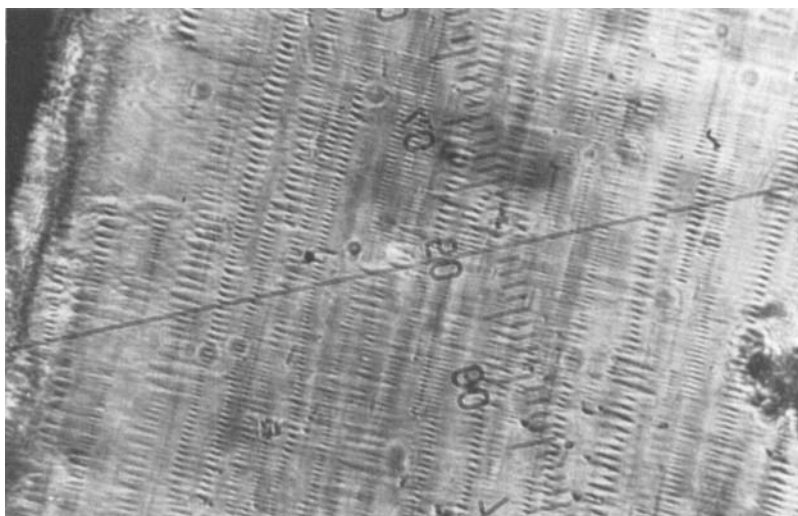


FIGURE 4 A confocal view of the regular arrays observed in a NPOB Sm A film 10 μ thick; $U = 700$ V, $f = 5$ kHz ($l = 1.5$ mm), initially crossed nicols, the electric field is along the nicol bisectrice; the polarizer then is rotated at an angle of 40°; the long side of the photo corresponds to 230 μ .

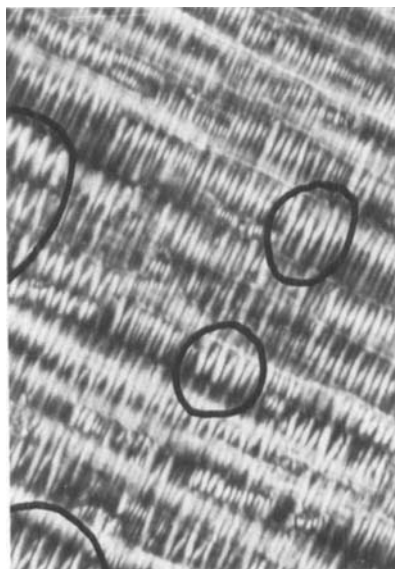


FIGURE 5 A view of the association of the focal conics from two adjacent arrays being marked in some regions in a NPOB Sm A film $10\ \mu$ thick; $U = 300\ \text{V}$, $f = 5\ \text{kHz}$ ($l = 2.5\ \text{mm}$), crossed nicols, the electric field is along the polarizer; the short side of the photo corresponds to $100\ \mu$.

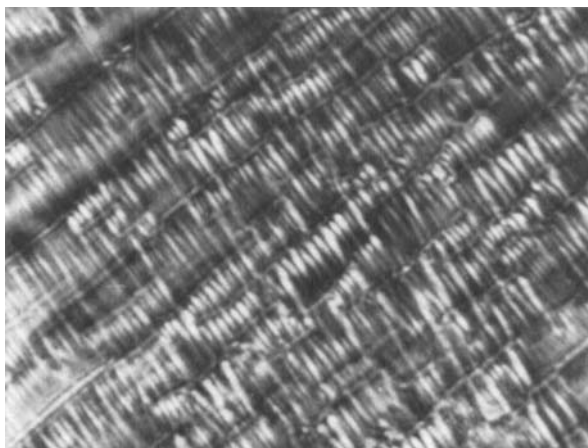


FIGURE 6 A view of the association of the focal conics from two adjacent arrays in some regions in a hybrid-aligned homeotropic-planar NPOB Sm A film $10\ \mu$ thick; $U = 200\ \text{V}$, $f = 5\ \text{kHz}$ ($l = 1\ \text{mm}$), crossed nicols, the electric field is along the polarizer; the long side of the photo corresponds to $150\ \mu$.

The voltage excitation of hybrid-aligned LC layers in both the N and Sm A phases gave very nice combined pictures of overlapping arrays of confocal domains situated near one of the electrodes and parabolic focal conics situated near the other electrode (Figure 7). These Sm A textures can also be seen without a polarizer (the removal of both nicols, however, permitted the observation of the focuses only). The change in the focal distance showed that the focal conics are situated on different levels near the two glass plates (see also Figure 4). The increase of the voltage from 200–700 V and the cell thickness from 10–50 μ did not significantly change the characteristic period of the ACD texture usually being in the range of 1–2 μ .

All the Sm A textures observed during our experimental study remained unchanged after the removal of the voltage.

Such Sm A textures consisting of arrays of focal conics can also be generated near the electrodes under the action of a strong nonhomogeneous electric field applied across the Sm phase only. In a voltageless state they can be created more frequently after K-Sm A phase transition upon heating (the parabolic focals existed at low temperatures, while nonregular arrays

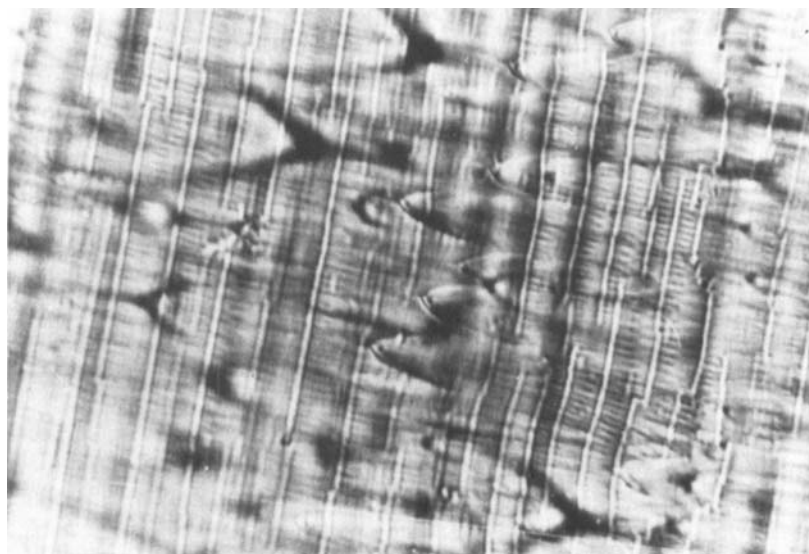


FIGURE 7 A combined picture of overlapping parabolic focals and regular arrays of confocal domains in a hybrid-aligned homeotropic-planar NPOB Sm A film 10 μ thick; $U = 500$ V, $f = 5$ kHz ($l = 1$ mm), crossed nicols, the electric field is along the nicol bisectrice; the long side of the photo corresponds to 230 μ .

of focal conics were generated at high temperatures in the smectic A interval) and very rarely after the N-Sm A phase transition upon cooling.

It is important to note that the arrays of confocal domains were more distinctly visible near the N-Sm A phase transition, whereas near the Sm A-K phase transition we observed the creation of many parabolic focals with a small size. It seems that the arrays of focal conics arise at once from the deformed nematic phase. No edge-dislocations or $\pm\pi$ disclinations were observed during the experimental investigations of initially homeotropic LC layers. However, it is important to stress that edge-dislocations were observed in hybrid-aligned cells exciting with low voltages below 200 V (the distance between the metal foils was around 1 mm) (Figure 8). Upon heating of a Sm A phase consisting of arrays of focal conics, the tails of the ellipses which represent the small deformed part of the smectic A disappeared first followed by the large curved heads. Consequently, the observed arrays of focal conics are a highly organized Sm A system consisting of a special arrangement of ellipses-hyperbolas with energy which is much lower than the energy of the edge dislocations or different kinds of grain boundaries.

III. DISCUSSION

To give a plausible interpretation of the Sm A textures observed it is necessary to know the possible ways for the eventual creation of regular arrays of focal conics. In accordance with Williams,²⁵ they can be created as a result of the competition between the forces, generated from the surfaces and the bulk forces due to electric and magnetic torques or by a hydrodynamic flow caused by slipping of the glass plates, etc. In all these cases, one can observe the creation of a number of one or half Grandjean's walls with parallel hyperbolas and an array of ellipses with equal eccentricity touching their heads and ends.^{25,26} Another very important and difficult problem is the filling of the available space with confocal domains^{13,14,25-29} and its solution requires the knowledge of the three main laws for the possible association of the focal conics: the law of the non-penetration of the focal conics, the law of the possible common generatrices of the focal conics and finally, the law of the corresponding cones (in effect, these laws had been discovered for the first time in 1910 by G. Friedel and F. Grandjean³⁰). In accordance with these laws and the possible surface orientation of the Sm A molecules, in respect to the orientation of the Sm A planes, the ellipses can be vertical, inclined or parallel relative to the glass plates (we will discuss only the possible position of the ellipses since the position of the hyperbolas can be easily determined in accordance

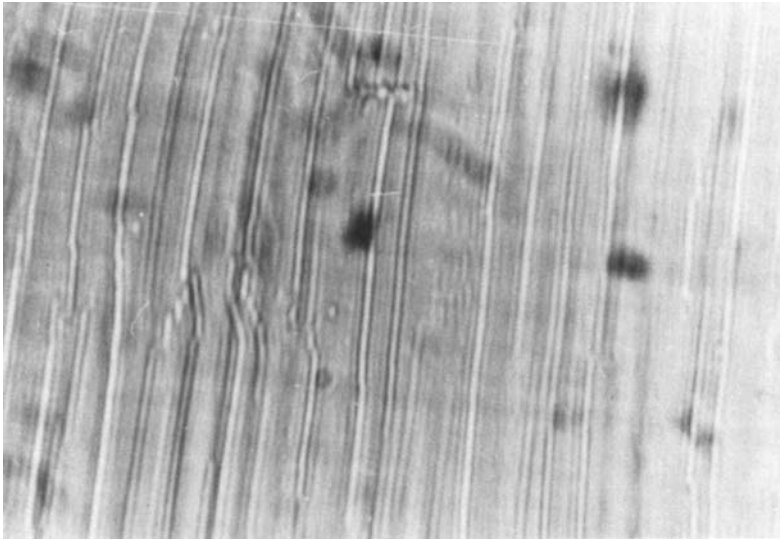


FIGURE 8 Edge-dislocations in a hybrid-aligned homeotropic-planar NPOB Sm A film $10\ \mu$ thick; $U = 150\ \text{V}$, $f = 5\ \text{kHz}$ ($l = 2.5\ \text{mm}$), crossed nicols, the electric field is along the nicol bisectrice; the long side of the photo corresponds to $230\ \mu$.

to the Dupen cyclide construction). Further, the ellipses can be situated on the glass plates or below and above them in the depth of the LC layer. They can be arranged in straight arrays touching their heads and ends and having equal eccentricity, or they can be arranged in curved arrays (or “treilles”). The plane association of the ellipses can be as follows: one array of parallel ellipses can be situated in one plane when they are equal in size and the touching is effected laterally (see Figure 4); two or more arrays of parallel ellipses can be situated in one plane only in the case of complete or half Grandjean’s walls²⁵ (in our opinion half Grandjean’s walls can exist only in cases when the ellipses are situated in the glass plates²); nonparallel ellipses can be situated in one plane only in the case of the so-called polygonal textures.^{25,30–34}

From our experimental results it is evident that the ellipses are regularly arranged in arrays, and we will be interested further in this arrangement only.

A. Arrays of confocal ellipses-hyperbolas with Marignan, Malet and Parodi arrangement

The careful comparison of the confocal arrangement obtained in our experiment which, as noted, is shown in Figures 5 and 6 with the confocal

arrangement observed by Marignan, Malet and Parodi^{10,11} in planar Sm A LC under shear (see Figure 8 in Ref. 10) as well as the considerations of these authors permitted us to understand that their interpretation for the confocal arrangement is valid for our case as well and to call this special arrangement of confocal domains adjusting the planar Sm A LC being in the middle part of the LC layer with the weakly anchored initially homeotropic or tilted Sm A LC which is in the boundary regions (Figure 9)—Marignan-Malet-Parodi confocal domain arrangement.

Let us discuss in more detail this arrangement of confocal domains. In effect, it consists of two opposite Grandjean's walls with ellipses which are inclined at angle θ to the glass plates and situated in two different levels and hyperbolas situated in such a way that two of the generatrices coincide (i.e. there is one common generatrix) and the other ones must be either normal to the outer Sm A layers where the molecules are parallel to the direction of the electric field or must be parallel to the glass plates (Figure 10). As claimed by Marignan and Parodi,¹¹ the ellipses from these two Grandjean's walls can cross each other since they are very elongated and their distorted parts are very small and located on opposite places (Figure 11). The careful scrutiny of the confocal arrangement shown in Figures 5 and 6 unambiguously pointed out that this is the case. On the other hand, this special arrangement of the confocal domains permits the easy adaptation of the normal Sm A layers which are in the middle part of the samples (planar position of the Sm A molecules which are parallel to the electric field) with the tilted position of the Sm A layers in the boundary regions since in such

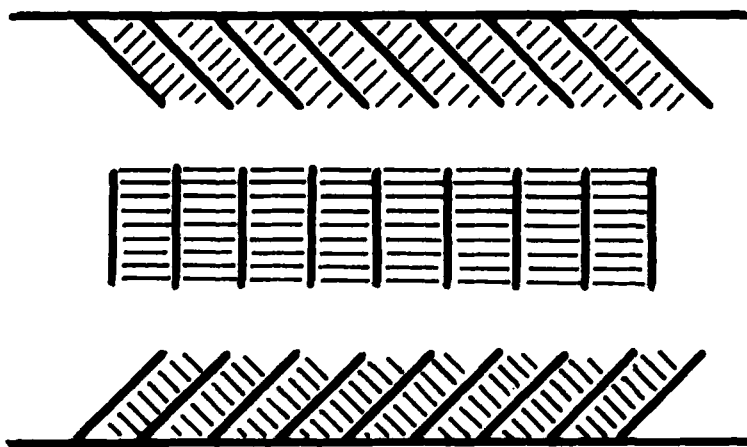


FIGURE 9 Schematic representation of the awaited orientation of the Sm A molecules and planes in the boundary regions and in the middle of the liquid crystal films under study.

an arrangement the surface energy is entirely overcome only along the generatrix of the upper cones situated near to the glass plates (Figure 10). In accordance to the association laws, the ellipses should be arranged in arrays situated on different levels into the LC and this arrangement was really confirmed in our experiment (Figure 4). In accordance with Marignan and Parodi¹¹ the higher density of ellipses is obtained when each cone has its apex on the following ellipse as shown in Figure 10 and as can be seen in some of the marked regions of Figure 5. As ellipses of each system are related by some translation operation and as can be seen on Figure 2, they form files aligned along the electric field direction; it follows that the external conical domains on each file must have a common horizontal generatrix.^{10,11}

The different sizes and eccentricity of the ellipses are probably due to the nonequal surface anchoring in the various regions of the LC area under

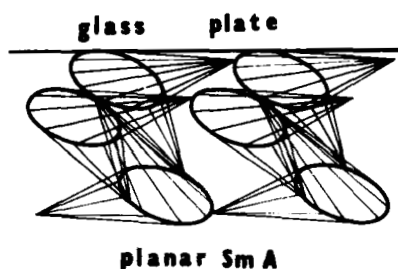


FIGURE 10 Marignan-Malet-Parodi association of the confocal pairs of ellipse-hyperbola; from the upper side is the glass plate, from the lower side is the planar Sm A LC.

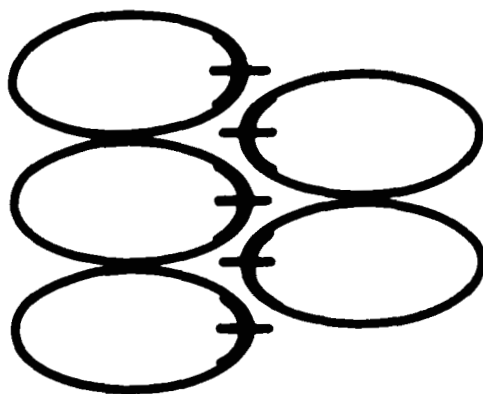


FIGURE 11 Schematic representation of the projection of crossed ellipses on the glass plate.

study and less probably to growing causes. It seems that most of the ellipses from two adjacent arrays cross each other as shown in Figure 10. Consequently, the region of the Sm A phase which is occupied by the heads of the ellipses consists of one bright line which is formed from the arrays of focuses and two black lines obtained from the overlapping of the ellipses situated on different levels of the LC.

In summary, the matching between the Sm A surface orientation in the glass plate vicinity which is highly tilted relative to the plane of the glass plates (before the confocal domain formation) and the Sm A bulk planar orientation of the molecules (a vertical position of the Sm A planes) is realized by creation of regular arrays of confocal ellipses-hyperbolas discovered for the first time by Marignan, Malet and Parodi^{10,11} in sheared planar Sm A films and consisting of two opposite Grandjean's walls. No optically observable regions with a complete planar orientation of the Sm A molecules were seen. This experimental finding is not very clear since the surface energy is not too large (see the calculated value given below) as confirmed by the absence of edge-dislocations or grain boundaries and by the very elongated shape of the ellipses observed. The filling of the available space is not clear as well. No additional confocal domains were observed. It seems that in the remaining space the surface energy is overcome and the Sm A molecules are planar (a vertical position of the Sm A planes).

B. Possible physical causes leading to the formation of regular arrays of focal conics in the Sm A phase

First, we shall accept that the Sm A textures observed are due in most of the cases to energetic causes and rarely to the growing ones. This is confirmed by the repeatable creation of the arrays of focal conics for different thickness of the LC films being changed between several microns and $50\ \mu$ and consequently for different temperature distribution (let us recall that the heating of the cells has been from below). On the other hand, these Sm A textures crucially depend on the LC surface orientation and anchoring as revealed by the repeatable appearance of the arrays of confocal domains in the same regions of the LC cells under study.

Second, the absence of grain boundaries, dislocation lines and $\pm\pi$ disinclinations^{25,27-29,35,36} unambiguously shows that the strength of the surface anchoring is not sufficient to support these highly energetic Sm A lines. As claimed by Williams,²⁵ the simple bending of the Sm A planes leading to grain boundaries is needed from a surface energy in the range of 4×10^{-2} erg/cm². In addition, our calculations based on the experimental observations of a number of grain boundaries obtained by Goscianski,

Lèger and Mircea-Roussel¹⁵ showed that the surface energy should be between 2×10^{-1} erg/cm² and 5×10^{-2} erg/cm² in order to support this kind of adjustment between the homeotropic alignment of the Sm A molecules at the boundaries and the planar alignment of the Sm A molecules in the middle part of the Sm A films. This shows that the surface energy of the Sm A LC NPOB under study interacting with a clean glass plate should be below 4×10^{-2} erg/cm². On the other hand, the observations of edge-dislocations in hybrid-aligned homeotropic-planar Sm A layers near to the glass plate treated by a thin SiO layer under vacuum evaporation to ensure the planar orientation of the Sm A molecules (Figure 8) clearly shows that the surface energy for this special case is in the range between 4×10^{-2} erg/cm² and 2×10^{-1} erg/cm², and this value has been confirmed by the experimental results obtained by Hinov² and Hochbaum and Labes.⁵ In addition, the low value of the surface energy and the absence of confocal arrays with a low eccentricity of the ellipses show that the type of the surface energy cannot ensure a Fréedericksz transition of a second kind (see also the results obtained by Goscianski *et al.*¹⁵): i.e. this energy is not of Rapini's type: $W_s \sin^2 \theta$, where W_s is the strength coupling constant and θ is the polar deformation angle.

C. Estimation of the total surface energy of the Sm A LC NPOB for the case of homeotropic alignment

Let us focus our attention to the Sm A phase arising from the strongly deformed nematic regions. It seems that the distribution of the arrays of confocal domains of different size and arrangement is directly related to the surface anchoring of the N and Sm A phases. In principle, one knows that the LC under study tends to align perpendicular to the glass plates.¹⁹ The existence of a well-defined Sm A surface energy is confirmed by the creation of well-defined Sm A local crystals with homeotropic orientation of the Sm A molecules and a planar position of the Sm A planes achieved after cooling of homeotropic Ns down to the Sm A phase. In addition, the Fréedericksz electric field threshold depends slightly on the thickness of the N layers under study. It is easy to calculate the surface energy of the N phase. It is more interesting however, to obtain the value of the surface energy of the Sm A LC because of both the absence of such measurements and its importance for the construction of Sm A LC cells for industrial applications. In our opinion, one should use Marignan-Malet-Parodi association of the focal conics constructed from two opposite Grandjean's walls (see Figure 10). On the other hand, we observed such regions as can be seen from Figures 5 and 6.

The total Sm A surface energy can be estimated from the theoretical results obtained by Kléman as a sum from the general curvature energy of a confocal pair of ellipse-hyperbola³⁷:

$$W_{cd} = K_1(1 - e^2)a \left\{ 4\pi K(e^2) \left(\ln \frac{a}{r_c} - 2 \right) + \int \frac{\ln e \cos v - \cos hu}{-e \cos v + \cos hu} du dv \right\} \quad (1)$$

where K_1 is the splay elastic coefficient, $K(e^2)$ is the complete elliptic integral of the first kind, e is the eccentricity of the ellipse, a is the half-length of the major axis of the ellipse, r_c is the core radius, u and v are the parameters describing the hyperbola and ellipse, respectively, and the core energy of the hyperbolic line:

$$W_{hl} = 2E_{cor}r \quad (2)$$

where E_{cor} is of the order of K_1 ¹⁴ and r in our case can be taken as a sum from the lengths of the two generatrices of the hyperbola (see Figure 11).

We are interested, however, only from the order of magnitude of the surface energy, since its exact calculation requires the knowledge for the filling of the remaining available space (see Figure 10). Consequently, we shall escape the numerical calculation of the integral being in the relation in Eq. 1 and shall use two approximate formulas showing the upper and lower limits of the value of the total surface energy:

$$W_s \int_0^{\theta_0} f(\sin^2 \theta) d\theta = \frac{l}{mn} \left\{ 4\pi K_1(1 - e^2)K(e^2)a_1 \ln \frac{a_1}{r_c} + 2E_{cor}r \right\} \quad (3)$$

$$W_s \int_0^{\theta_0} f(\sin^2 \theta) d\theta = \frac{l}{mn} \left\{ 2\pi K_1 a \left(\ln \frac{2a}{r_c} - 2 \right) + 2E_{cor}r \right\} \quad (4)$$

respectively, where l is the number of the confocal pairs, m and n are the lengths in centimeters of the chosen parallelepiped which contains the confocal domains under study, a is the focal length of the ellipses given by the following formula:

$$a = a_1 - (a_1^2 - b_1^2)^{1/2} \quad (5)$$

where b_1 is the minor axis of the ellipse. Let us stress that in the latter formula we use the nice interpretation of the observed pairs of ellipses-hyperbolas as slightly deformed spheres given by Marignan and Parodi.¹¹

For numerical calculations we use one of the marked regions shown in Figure 5 with the following numerical data: $a_1 = 5 \mu\text{m}$, $b_1 = 3 \mu\text{m}$, $e = 0.8$, $r_c = 100 \text{ \AA}$, $r = 24 \mu\text{m}$, $E_{cor} = K_1$, $m = 23 \mu\text{m}$, $n = 6 \mu\text{m}$

and $l = 4$. The calculations gave the following range of the possible value of the total surface energy for the chosen region:

$$0.3 \times 10^{-2} \text{ erg/cm}^2 < W_s \int_0^{\theta_0} f(\sin^2 \theta) d\theta < 0.9 \times 10^{-2} \text{ erg/cm}^2 \quad (6)$$

Consequently, the real value of the total surface energy is in the range of

$$W_s \int_0^{\theta_0} f(\sin^2 \theta) d\theta \approx 5 \times 10^{-3} \text{ erg/cm}^2 \quad (7)$$

This value of the surface energy is one order of magnitude lower relative to the surface energy which is needed for the creation of grain boundaries or $\pm\pi$ disclinations (see the estimations of these energies given above). So the surface torques determined by this small surface energy are too weak to support the creation of edge-dislocations or $\pm\pi$ disclinations, and this was unambiguously confirmed in our experiment.

Let us note that our experimental results showed nearly the same surface energy for a Sm A LC NPOB interacting with a glass plate coated with lecithin. Moreover, this value of the surface energy is typical for the interface homeotropic NPOB Sm A LC, a clear or lecithin-coated glass plate, and cannot be accepted for a final order of magnitude of the surface energy of the various homeotropic Sm A LCs. It is clear that this energy will vary with the nature of both the glass plates and their coating and the very Sm A LC.

The maximal tilt angle θ_0 can also be calculated according to the formula given by Williams²⁵:

$$\theta_0 = 2\theta = 2\text{arccotg}(a_1^2/b_1^2 - 1)^{1/2} \quad (8)$$

and is varied between 72° for the chosen pairs of confocal ellipse-hyperbola utilized in the numerical evaluation of the surface energy (see Figure 5) and 10° – 20° for the more elongated ellipses. On the other hand, it is clear that the surface tilt varies between this value and zero (planar orientation of the Sm A molecules) along the generatrices of the hyperbolas touching the glass plate.

IV. CONCLUSIONS

A Sm A NPOB LC was obtained after cooling of homeotropic and hybrid-aligned homeotropic-planar N layers subjected to the action of a transversal high-frequency electric field. At low voltages (in respect to electric fields)

$$1.5E_{th} \leq E \leq 3E_{th}$$

the textures obtained were in agreement with Cladis and Torza's experimental results for hybrid-deformed layers.¹ At higher electric fields, the matching between the surface homeotropic (or slightly tilted) orientation and the bulk planar orientation of the Sm A molecules produced a number of regular arrays of confocal pairs of hyperbola-ellipse consisting of two opposite Grandjean's walls. The size and the association of these arrays of focal-conics can be very different and are determined by the strength of the surface coupling. Such an arrangement has already been observed and clarified by Marignan, Malet and Parodi^{10,11} in sheared planar Sm A films. This special arrangement permitted the approximate calculation of the total mean surface energy of a homeotropic NPOB Sm A LC film interacting with a clean or lecithin-coated glass plate which is in the range of 5×10^{-3} erg/cm². The value of this energy is much lower relative to the surface energy of planar Sm A layers and cannot support the creation of grain boundaries or $\pm\pi$ disclinations.

All the Sm A textures observed during our experimental investigations remained unchanged after the removal of the voltage. They might be applied either as strong-scattering textures with a longtime stability when the arrays of focal conics are strongly nonregular or as diffraction gratings when the arrays of focal conics are well-aligned.

Although many kinds of arrays of focal-conic domains were obtained, we have considered only those pictures which are both typical and of some use for the determination of the surface energy which is important for the experimental research and for a technical application of the Sm A LC.

References

1. P. E. Cladis and S. Torza, *J. Appl. Phys.*, **46**, 584 (1975).
2. H. P. Hinov, *J. Physique*, **42**, 307 (1981).
3. H. P. Hinov and M. Petrov, *Mol. Cryst. Liq. Cryst.*, in press (1983).
4. I. Janossy and L. Bata, KFKI-65 (1977).
5. A. Hochbaum and M. M. Labes, *J. Appl. Phys.*, **53**, 2998 (1982).
6. J. E. Proust and E. Perez, *J. Physique Lett.*, **38**, L-91 (1977).
7. E. Perez and J. E. Proust, *J. Physique Lett.*, **38**, L-117 (1977).
8. W. H. Chu and J. T. Jacobs, *IBM J. Res. Dev.*, **22**, 40 (1978).
9. E. Meirovitch and J. H. Freed, *J. Phys. Chem.*, **84**, 2459 (1980).
10. J. Marignan, G. Malet and O. Parodi, *Ann. Phys.*, **3**, 221 (1978).
11. J. Marignan and O. Parodi, *J. Physique Colloq.*, **40-C3**, C3-78 (1979).
12. A. N. Nesrullaev and A. S. Sonin, *Zh. Phys. Chim.*, **LIII**, 2481 (1979).
13. O. Parodi, *Sol. St. Comm.*, **11**, 1503 (1972).
14. R. Bidaux, N. Boccara, G. Sarma, L. de Seze, P. G. de Gennes and O. Parodi, *J. Physique*, **34**, 661 (1973).
15. M. Goscianski, L. Léger and A. Mircea-Roussel, *J. Physique Lett.*, **36**, L-313 (1975).
16. D. Langevin, *Phys. Lett.*, **56A**, 61 (1976).
17. D. Langevin, *J. Physique*, **37**, 755 (1976).
18. Ch. S. Rosenblatt, R. Pindak, N. A. Clark and R. B. Meyer, *J. Physique*, **38**, 1105 (1977).

19. D. Demus, H. J. Deutscher, S. König, H. Kresse, F. Kuschel, G. Pelzl, H. Schubert, Ch. Selbmann, W. Weissflog, A. Wiegeleben and J. Wulf, "Forschungen über Flüssige Kristalle . . . 1. NPOB," Ed. D. Demus, Martin-Luther-Universität, Halle-Wittenberg, Wiss. Beiträge, **21**, 9 (1978).
20. L. E. Hajdo and A. Cemal Eringen, *J. Opt. Soc. Am.*, **69**, 1017 (1979).
21. M. I. Barnik, S. V. Beljaev, V. G. Rumjanzev, V. A. Zwetkoff and N. M. Shtikov, "Forschungen über Flüssige Kristalle . . . 1. NPOB," Ed. D. Demus, Martin-Luther-Universität, Halle-Wittenberg, Wiss. Beiträge, **21**, 84 (1978).
22. A. Köler, "Forschungen über Flüssige Kristalle . . . 1. NPOB," Ed. D. Demus, Martin-Luther-Universität, Halle-Wittenberg, Wiss. Beiträge, **21**, 95 (1978).
23. F. Scudieri, *Ann. Phys.*, **3**, 311 (1978).
24. P. E. Cladis, *J. Physique Colloq.*, **37**, C3-137 (1976).
25. C. E. Williams, Ph. D. Thesis, Université de Paris-Sud, Orsay (1976).
26. M. Hareng, S. Le Berre and J. J. Metzger, *Appl. Phys. Lett.*, **27**, 575 (1975).
27. C. E. Williams, *J. Physique Colloq.*, **39**, C2-46 (1978).
28. C. E. Williams and M. Kléman, *J. Physique Colloq.*, **36**, C1-315 (1975).
29. C. E. Williams and M. Kléman, *J. Physique Lett.*, **35**, L-33 (1974).
30. G. Friedel and F. Grandjean, *Bull. Soc. Franc. Miner.*, **33**, 409 (1910).
31. Y. Bouligand, *J. Physique*, **33**, 525 (1972).
32. Y. Bouligand, *J. Microscopie*, **17**, 145 (1973).
33. M. Kléman, "Points. Lignes. Parois," *Les Editions de Physique*, France (1977).
34. Y. Bouligand, *J. Physique*, **34**, 603 (1973).
35. P. G. de Gennes, *Sol. St. Comm.*, **10**, 753 (1972).
36. P. G. de Gennes, *C. R. Acad. Sc. Paris*, **275**, 549 (1972).
37. M. Kléman, *J. Physique*, **38**, 1511 (1977).